

Analysis of some flow parameters around a Magnus wind turbines models

Anastas Yangyozov¹, Zhivko Zhekov², Krastin Jordanov¹, Daniela Chakyrova¹, Nadezhda Doseva¹

1 – Technical University of Varna, Department of Thermal Engineering, 9010, 1 Studentska Street, Varna, Bulgaria

2 – Technical University of Varna, Department of Industrial Automation, 9010, 1 Studentska Street, Varna, Bulgaria

Corresponding author contact: yangyozovtu@tu-varna.bg

Abstract. *The present work presents the results of an experimental study of models of air turbines operating with the Magnus effect with a horizontal and a vertical axis of rotation. Pressure and velocity were measured with wireless data transfer equipment. Model air turbines are described and their main geometrical dimensions are presented. The experiments were done in a wind tunnel, and the working models were tested with different numbers of rotating cylinders. The problems in creating the small turbines and the limitations in their operation are discussed.*

Keywords: Magnus effect, vertical axis wind turbine, horizontal axis wind turbine, experiment, turbulence flow

1 Introduction

Any specialist engaged in power engineering would ask himself or herself the question what would be the role of the renewable energy sources, and more specifically, of the wind farms in the future for the electrical energy production. Currently, the use of renewable energy sources cannot replace the thermal power plants, the hydro-power plants or the nuclear power plants. The power engineering on a global scale is facing a major challenge. The Magnus effect is an unconventional method for extracting the energy of a moving fluid. Nowadays there is not much information about these relatively new wind turbine designs. Experimental data on actual operating models or units is not available, and the published data is incomplete and fragmentary.

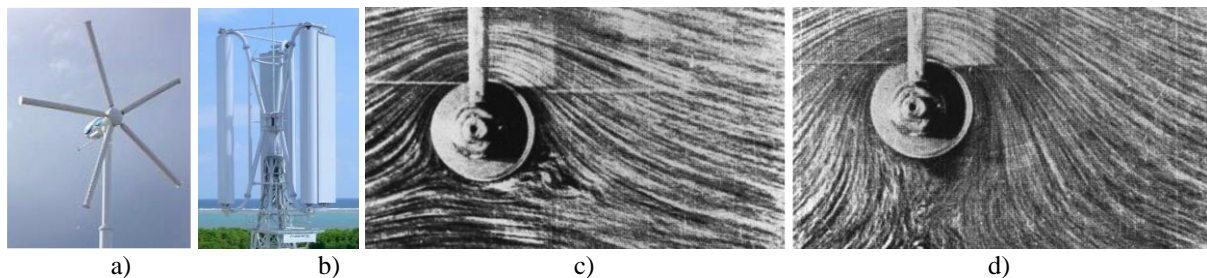


Fig. 1. Magnus turbines working in practice (a) HAMWT (Ikezawa, 2018), (b) VAMWT (Challenergy, 2024) and (c),(d) streamlines around rotating cylinders (Prandtl, 1934 and Anderson, 2011).

In 2007, specialists from the company “MECARO“, Japan (Ikezawa, 2018) elaborated and proposed on the energy market a horizontal axis wind turbine (HAMWT), applying the Magnus effect.

Nowadays, engineers from the company “Challenergy“, Japan (Challenergy, 2024) are successfully implementing in practice vertical axis wind turbines (VAMWT), which are not influenced by the wind direction. In 2018, in Japan, on the Okinawa Island, a three-cylinder prototype was presented, producing electric power of 10kW with wind velocity up to 30.4m/s (109km/h) (Challenergy, 2020). In 2021, on the Batan Island in the Philippines, a two-cylinder turbine was launched into operation, where according to the calculations, presented in (Limpot, 2023) and the data in (Challenergy, 2024), the unit is capable of generating power of 10 kW with 11m/s up to 176.79kW with 40m/s. The latter shows that those wind turbines are capable of working also in a hurricane wind, i.e. with 144 km/h.

One of the reasons to pay special attention on that type of turbines is their smaller size compared to the classical horizontal axis turbine with fixed blades with the same power. According to (Borg, 1986) the turbines working with the Magnus effect are compact and with a high torque. The small size of the Magnus turbines also leads to a low level of generated noise. With VAMWT (see Fig.1,b) the noise level at work is 52dB (Challenergy, 2024). In Lukin scientific work (Lukin, 2022), HAMWT is considered. The study has been performed with a high precision measuring equipment. In this experimental work the operating curves of the HAMWT were obtained.

Using the theoretical connections, described in (Bohl, 2005), allows to draw conclusions which parameters have an impact on the raising lift force F_A . According to Kutta–Joukowski theorem, the lift force of an airfoil with a circular cross-section is given by

$$F_A = 2 \cdot \pi \cdot \rho \cdot b \cdot V \cdot \omega \cdot r^2 \quad (1)$$

where, ρ -flow density; b -cylinder length; V -flow velocity at cylinder inlet; ω -cylinder angular velocity; r -cylinder radius.

In order to study more precisely the phenomena in the rotating frame with rotors, it is advisable to apply the advanced tools of the computational fluid dynamics (CFD). Currently, there are only a few publications related to the attempts for numerical modeling of three-dimensional flow around rotating cylinders in turbines, working with the Magnus effect (Limpot, 2023), (Sakipova, 2019), (Tanasheva, 2021), (Ogawa, 2018). With the CFD calculation of Magnus turbines, some problems arise that are related to the modeling of eddy structures. Regardless of the success achieved over the recent years in the field of numerical modeling, the calculation of the characteristics of vortex flow around rotating cylinders has proven to be an uneasy task, mainly due to the fact that this is a transient problem.

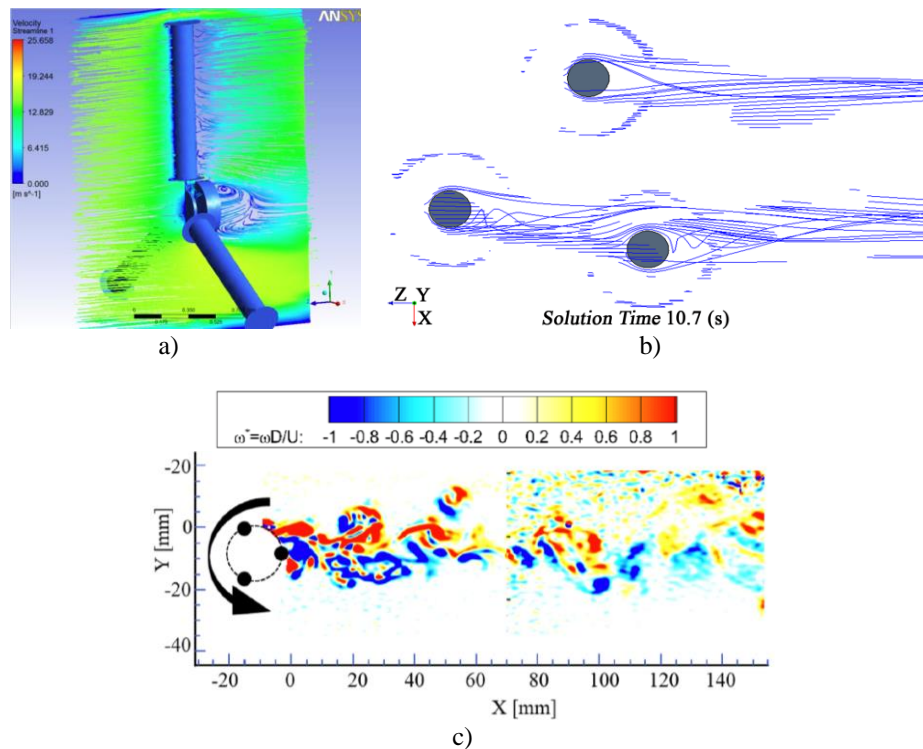


Fig. 2. Streamlines around HAMWT and VAMWT, obtained by CFX and Fluent software (a) (Sakipova, 2019), (Tanasheva, 2021), (b) (Ogawa, 2018) and (c) vortex structures after VAMWT, obtained experimentally (Al Habib Ullah, 2022).

Modeling in the environment of the available CFD software products is difficult, yet it is not impossible. The software module CFX, for example, does not have ready-made tools, whereby a model can be created quickly and easily, and be studied in the virtual environment. The advantages of the GUI-method cannot be used. Programs need to be written in order to complete the standard code, which takes

time and requires user's skills. The software module Fluent allows having this task solved, where modeling is easier than in CFX. The difficulties in modeling are related to defining two or more coordinate systems, which are positioned differently in space and have different number of revolutions. The problem is transient and requires significant computational resource. The visualization with smoke in combination with CFD could in the future explain the reason for the generation and the frequency of appearance of vortices with particular dimensions. The measurements show that after the rotating components the flow is filled with unsteady and incoherent vortices (see Fig.2c, Al Habib Ullah, 2022). The vortex shedding after the rotating frame is studied in the work of AlUllah, however, it does not become clear what is happening in the core of the rotating fluid domain, closely after the cylinders. No detailed picture can be obtained at present, nor the number of the vortex structures may be known, or understand their influence on the work of the rotating cylinders. The problem is complicated due to the eddy structure of the flow in the rotating fluid region. The current article presents some results from an experimental study of HAMWT and VAMWT models conducted in the laboratory "Hydro- and Aerodynamics" at the Technical University – Varna.

2 Description of the experimental arrangement, the measuring devices and the structures of the HAMWT and VAMWT models

2.1 Description of the experimental arrangement

Fig.3 represents a scheme of the experimental arrangement used for determining some of the aerodynamic parameters of the air turbines.

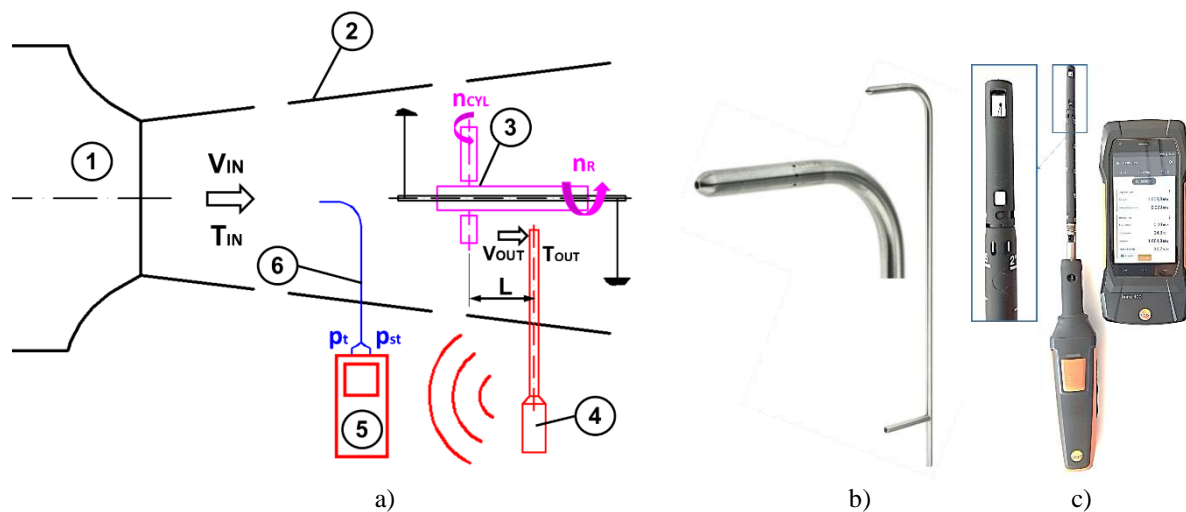


Fig. 3. Experimental arrangement scheme (a) and measuring tools used during the tests (b), (c).

The main components of the experimental arrangement are: 1-wind channel outlet, 2-wind channel jet, 3-air turbine, 4-Testo hot wire probe, 5-Universal IAQ instrument Testo 400, 6-Pitot tube.

The air is conducted to the inlet of the rotating frames with a nozzle (see Fig.3,a), installed at the outlet of the wind channel for the needs of the experiment.

2.2 Experimental tools description

The following measuring tools are used for measuring the aerodynamic parameters of the air:

- Pitot tube for measuring the air velocity before the turbine models using total and static pressure. Length 500mm, \varnothing 7mm (see Fig.3,b);
- Universal IAQ instrument Testo 400 (see Fig.3,c), accuracy according (Testo, 2022);
- Testo Hot Wire Probe Head for measuring the velocity after the rotating cylinders (see Fig.3,c), accuracy according (Testo, 2023);

- Digital tachometer DT-2234A for measuring the number of revolutions of the turbine shaft n_R , accuracy according (DT Operational manual).

Data about p_{st} , p_t , T_{IN} is measured and recorded with the Pitot tube and Testo 400 at a point after the aerodynamic canal, i.e before the air turbine. The V_{IN} values are calculated via the measured data, which do not change but remain constant for the current mode of operation. This indicates that the aerodynamic canal provides constant air flow parameters at the inlet of the tested air turbine. No such condition is observed after the rotating model of HAMWT/VAMWT at a selected point at a distance L (see Fig.3,a). Flow is turbulent there, and the flow parameters are changing over time. The Testo Hot Wire Probe Head (see pos.4 Fig.3,a) is used for measured air velocity data after the rotating cylinders. It is positioned after the cylinders at a distance $L=150\text{mm}$, and at the height of 50% of the cylinder length. The body of the probe is firmly attached to a fixed stand. Then the fan of the aerodynamic canal is started, the turbine cylinder rotation is started. The rotor speed slowly increases until a constant value is established. The velocity before the air turbine is measured with a Pitot tube (see pos.6 Fig.3,a) for three regimes with three different velocities V_{IN} , data recording in Testo 400 is started (see pos.5 Fig.3). The data is transmitted wirelessly. The sent values for p_{st} , p_t , T_{IN} , V_{OUT} , T_{OUT} are recorded and stored in the Universal IAQ instrument until the end of the measuring. Then the Testo 400 software generates a table with information about the test, which is sent to the user email or to a smart phone. Equipment for determining the torque on the shaft of the two turbines is to be purchased. This is an issue, which has been examined in detail by (Tujarov, 2016) and (Ahmedov, 2013).

2.3 Description of the HAMWT and VAMWT models

The first step is creating virtual three-dimensional geometric models in the module Design Modeler of ANSYS Workbench. The second step is realized with the assistance of the Cura software in preparation for three-dimensional printing. The turbine construction includes the following main stages:

- three-dimensional models creation;
- preparing the models for 3D printing;
- printing;
- cleaning and additional processing;
- assembling;
- setting;
- testing.

The time for printing varies from one to six hours in respect to the complexity of the three-dimensional form of the turbine components and the settings embedded in Cura.

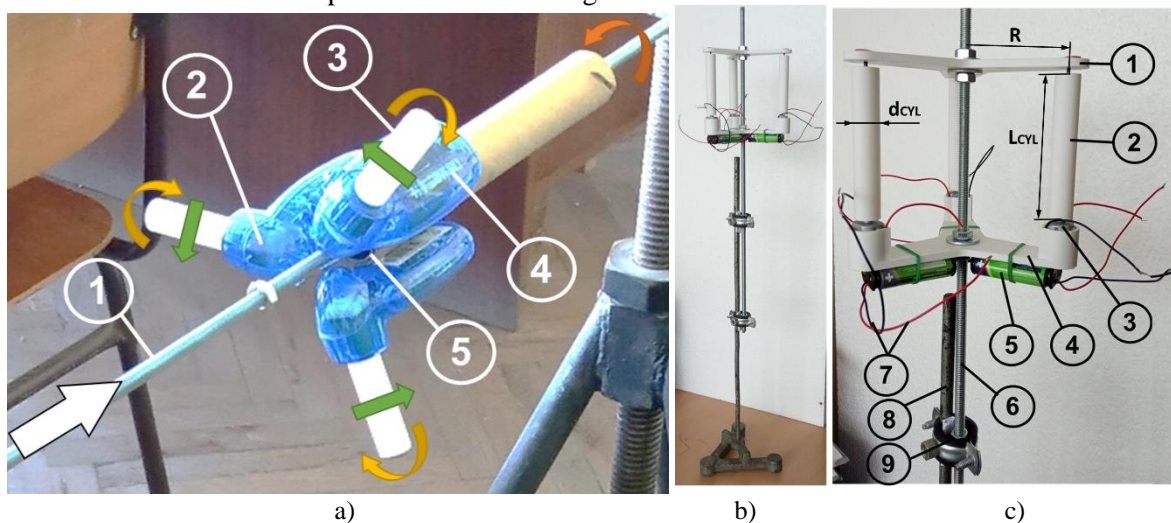


Fig. 4. Functional model of HAMWT (a) and model of VAMWT (b),(c) with main components.

Fig.4 presents the produced air turbine models with the main components and fixed stand, as follows. Figure 4,a shows the main components of HAMWT rotating frame: 1-shaft, 2-electrical motor, 3-rotat-

ing cylinder, 4-source of electrical power, 5-support frame with bearing. The main geometric dimensions of HAMWT are: wheel radius $R=100\text{mm}$; cylinder diameter $d_{\text{CYL}}=16\text{mm}$; cylinder length $L_{\text{CYL}}=50\text{mm}$, shaft number of revolutions $n_R=70\text{-}290\text{min}^{-1}$. Figure 4,b and c presents the main components of VAMWT rotating frame: 1-top frame, 2-rotating cylinder, 3-electrical motor, 4-lower frame, 5-source of electrical power, 6-shaft, 7-electrical wires, 8-support rod, 9-bearing. The main geometric dimensions of HAMWT are: radius of rotation $R=70\text{mm}$, cylinder diameter $d_{\text{CYL}}=16\text{mm}$; cylinder length $L_{\text{CYL}}=90\text{mm}$, shaft number of revolutions $n_R=60\text{-}340\text{min}^{-1}$.

When manufacturing VAMWT, there is added some elastic material – rubber, or aeroplast polyethylene in the cups of the lower frame (see the cup at end of position 4 on Fig.4,c) before assembling the electric motors. If that is not done, the electric motors will start vibrating, and the connection between the shaft and the cylinder hub will be damaged.

In the third step, the models are assembled and tested in an aerodynamic canal. The first main goal is to check the operating capacity of the wind turbines, to make sure that they will function with different inlet air velocities. The second goal is to measure some air flow parameters before the turbines, and in the eddy shedding, after the rotor.

3 Results and discussion

There are six physical models developed within the project, one of horizontal axis unit and five of vertical axis unit, by using the Magnus effect. Some of the models proved to be a dysfunctional structure, so they were disassembled and their components were used for creating turbines with an improved design.

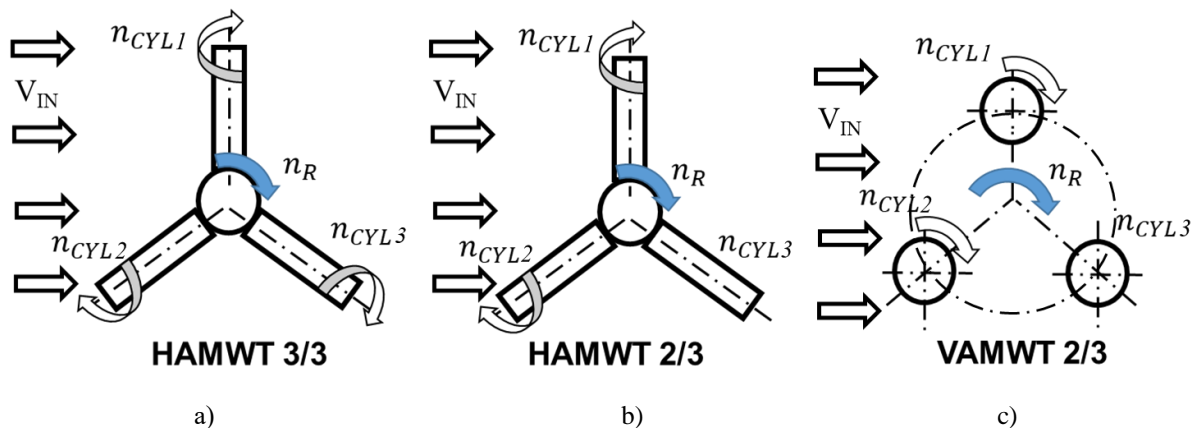


Fig. 5. Schematic representation of the tested turbine models rotors.

Figure 5 schematically presents the tested models of HAMWT and VAMWT. The rotational speed of the cylinders n_{CYL} does not change while the rotational speed of the rotor n_R changes with the air velocity V_{IN} .

The trials are organized in two groups: of the models of HAMWT (fig.5,a and b) and of VAMWT (fig.5,c). The following encoding of the abbreviations is introduced within the analysis:

-HAMWT3/3-horizontal axis Magnus turbine with three rotating cylinders of three in total, mounted on the rotor;

-HAMWT2/3-horizontal axis Magnus turbine with two rotating cylinders of three in total, mounted on the rotor;

-VAMWT2/3 should be read as a vertical axis turbine with two rotating cylinders of three in total.

The velocity at the outlet of the wind channel, respectively, at the inlet of the rotating frame, is maintained constant for the current regime $V_{\text{IN}}=3.4\text{m/s}\text{-}8.0\text{m/s}$. Those velocities at the inlet of HAMWT and of VAMWT are changed during the tests by control of wind channel electrical motor with an inverter.

3.1 Modes of operation of HAMWT with operating three cylinders out of three, as well as with two out of three cylinders

Nest stage is HAMWT testing. Some of the HAMWT models were destroyed during the trials, and, some new ones had to be made. The reason was high speed rotor. That happened with velocity at the inlet of $V_{IN} > 5\text{m/s}$ and rotor number of revolutions $n_R > 300\text{min}^{-1}$. The air velocity at the turbine inlet was then reduced. After that no problems have been observed during the operation of HAMWT. They always start smoothly and work without problems.

Before starting the trials, the following simple test for the presence of the Magnus effect should be done. If the cylinder rotation is stopped from the electric motors ($n_{CYL} = 0\text{min}^{-1}$), there will be no Magnus effect, nor any rotation of the shaft ($n_R = 0\text{min}^{-1}$). When cylinders (two or all three) increase revolutions n_{CYL} the shaft will gradually increase the number of its revolutions n_R . Measuring starts as soon as the mode of operation is established.

The measured data for HAMWT at different working conditions are presented in Table 1.

Table 1. Measured data for HAMWT.

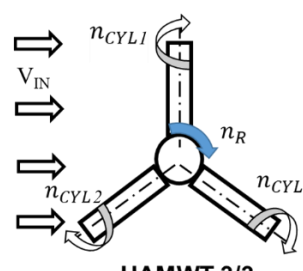
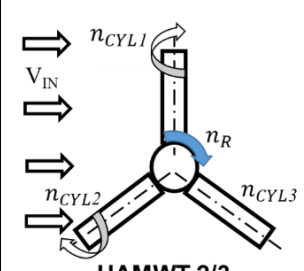
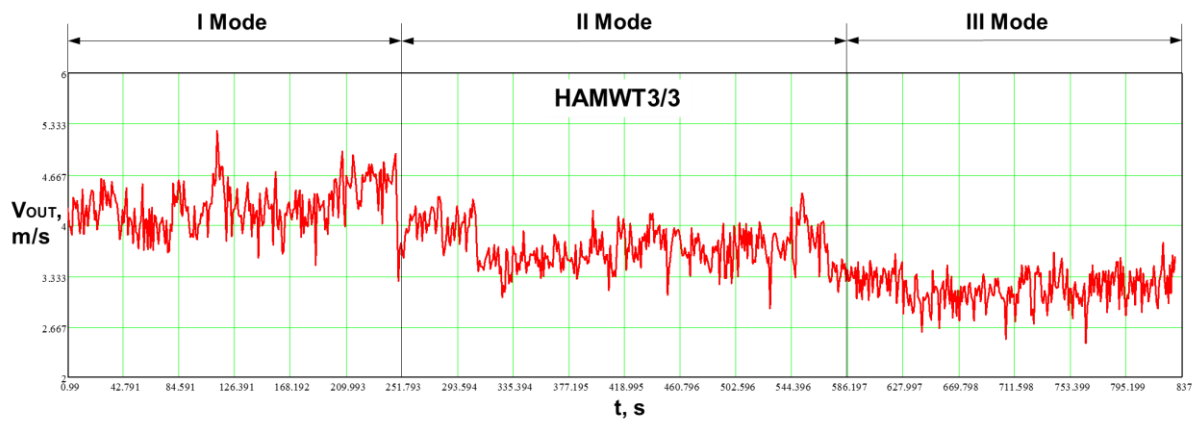
Schematic representation of test rotor	 <p>HAMWT 3/3</p>			 <p>HAMWT 2/3 $n_{CYL3} = 0\text{min}^{-1}$</p>		
	Mode	I	II	III	I	II
$V_{IN}, \text{m/s}$	4.6	4.0	3.4	4.6	4.0	3.4
n_R, min^{-1}	285	249	160	207	143	74

Fig. 6,a presents the measured data about the velocity after the rotating frame V_{OUT} with three rotating cylinders of HAMWT. At the moment of time 251.8s, the velocity at the turbine inlet V_{IN} changes from 4.6m/s to 4.0m/s, while at the moment of 586.1s, the velocity at the inlet V_{IN} changes from 4.0m/s to 3.4m/s. The digital tachometer measures the number of revolutions of the rotor n_R , which carries the rotating cylinders.

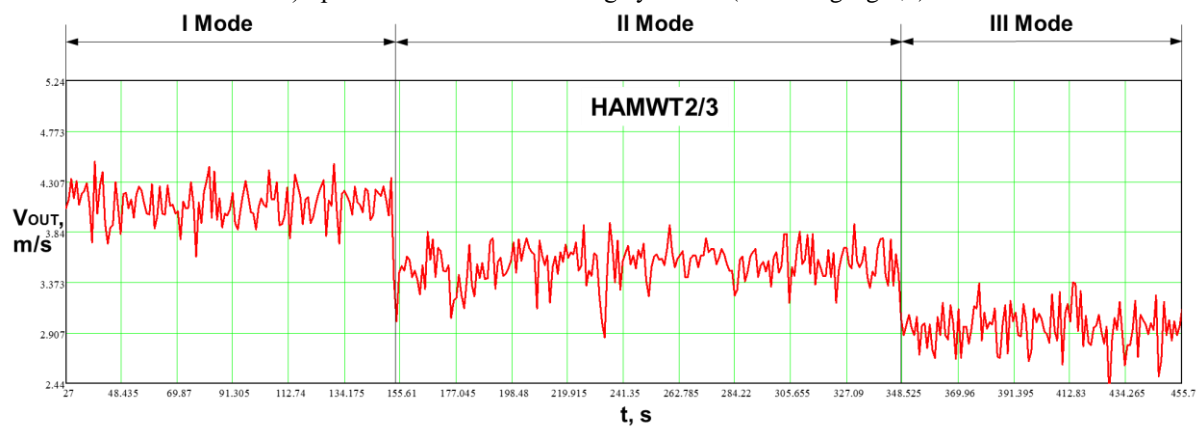
The next group of measurements is conducted after turning off the rotation of one cylinder of the three working ones. Fig. 6,b presents the measured data about the velocity after the rotating frame V_{OUT} with two rotating cylinders of HAMWT. At the moment of time 254.1s, the velocity at the turbine inlet V_{IN} changes from 4.6m/s to 4.0m/s, while at the moment of 348.4s, the velocity at the inlet V_{IN} changes from 4.0m/s to 3.4m/s.

It is evident from the obtained data about the velocity V_{OUT} , visualized on fig. 6, that in the flow after the rotor 3 at a distance L (see Fig. 3,a) there are vortices generated. The streamlines pattern changes over time, where an indicator for that is the instantaneous change of the velocity V_{OUT} , when there are three working cylinders (see Fig. 6,a). With two working cylinders (fig. 6,b), the data about the velocity is oscillating with about one average value for the current mode of operation, i.e. the change in V_{OUT} is smaller over time compared to the previous case shown in fig. 6,a.

The minimum value of the air velocity at the inlet for testing the HAMWT model is 3.4m/s, while the maximum is 5m/s.



a) operation with three working cylinders (according fig.5,a)



b) operation with two working cylinders (according fig.5,b)

Fig. 6. Measured air speed after HAMWT with three (a) and with two (b) rotating cylinders for three operating modes with inlet speed $V_{IN}=4.6\text{m/s}$, 4.0m/s and 3.4m/s .

3.2 Modes of operation of VAMWT with operating two out of three cylinders

The next stage in the project is focused on testing the VAMWT. The complex design of the model led to problems in the frames design supporting the rotor components (see position 4 Fig.4,c). The friction in the supports was reduced by adding high-quality bearings and a lubrication oil at the problem points.

The first VAMWT experimental unit did not function according to the expectations, therefore they had to be remanufactured by changing the ratio radius of rotation/cylinder diameter (R/d_{CYL}). Some uneven operation with pulsations has been observed with other VAMWT models. The reasons are discussed in the text below.

Table 2. Measured data for VAMWT.

Schematic representation of test rotor			
	Mode	I	II
$V_{IN}, \text{m/s}$	8.0	6.8	4.6
n_R, min^{-1}	337	99	72

The flow conditions and the data for this experiment are presented in Table 2 with schematic view of VAMWT rotor and measured parameters.

Fig. 7 presents the measured data, collected by Testo 400 Universal IAQ instrument for the velocity after the rotating frame V_{OUT} of VAMWT. The test is made with two rotating cylinders. At the moment of time 282.6s, the velocity at the turbine inlet V_{IN} changes from 8.0m/s to 6.8m/s, while at the moment of 524.2s, the velocity at the inlet V_{IN} drops below 6.8m/s.

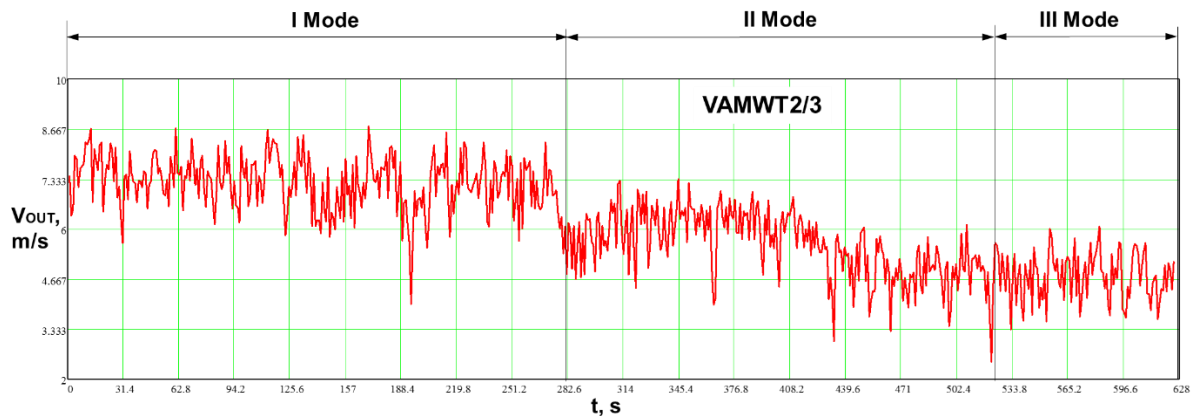


Fig. 7. Measured air speed after VAMWT with two rotating cylinders for three modes of operation (acc. fig.5,c).

In HAMWT2/3, the speed values V_{OUT} oscillate around the average values for all operating modes (see fig.6,b). In second operating mode of VAMWT2/3, a strong change in speed V_{OUT} is observed (see fig.7). That shows VAMWT2/3 operates in a complex turbulent unsteady flow.

Some of the models failed to start revolving due to fact that the vortices influence negatively the work of some rotating cylinders, and they do not create a Magnus force, respectively, a torque, which should produce useful power. How this negative effect can be influenced? It was established within the project that if the radius of rotation R is increased the influence of the vortex structures will be reduced, however, the large radius leads to increasing the dimensions of the turbine. Increasing the cylinder length L_{CYL} , in combination with a moderate radius R , will generate a greater Magnus force. The relations d_{CYL}/R and L_{CYL}/R are taken into account until reaching the final structure of the VAMWT model (see Fig.4,b and c). The minimum value of the air velocity at the inlet for testing the VAMWT model is 4 m/s, while the maximum is 8 m/s.

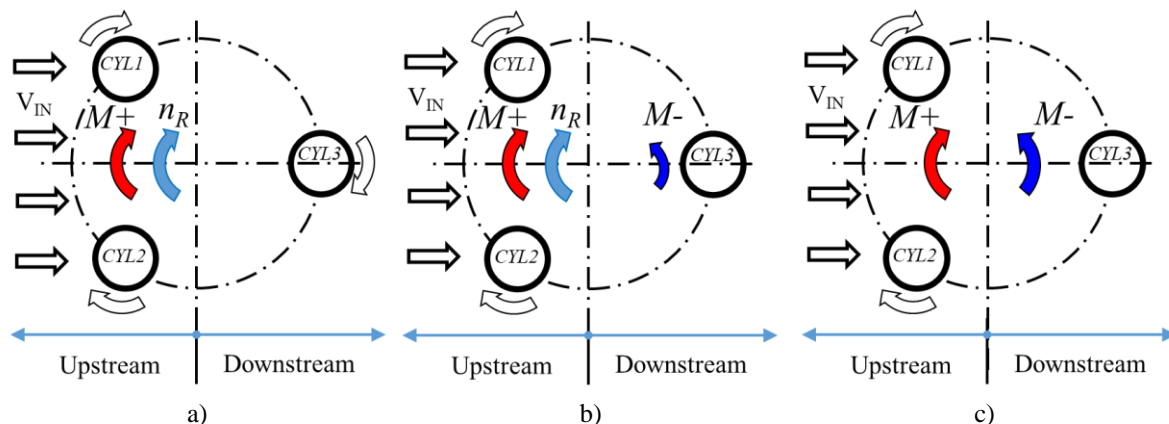


Fig. 8. Different scenarios of VAMWT operation.

In effective mode of operation the rotating cylinders produce a high Magnus force, resulting in a high positive torque $M+$ (fig.8,a). The vortex tracks influence the air flow across the cylinders situated in the second half of the rotating frame (the downstream rotor half). Vortex generation is inevitable since there are cylinders rotating in the structure (fig.2,c). When air flow across the VAMWT with two rotating

cylinders (fig.8,b), after the rotor there is an unsteady turbulent flow observed. There are regimes with model operation where there is positive work done from the upstream half (torque M_+) and negative work from the downstream half (M_-), see fig.8,b and c. That leads to reducing the obtained useful work of the turbine shaft and in some cases the torque generated at the rotor shaft is insignificantly small and the rotor does not rotate (fig.8,c $n_R=0\text{min}^{-1}$), or rotates with very small revolutions (fig.8,b $n_R\approx 0\text{min}^{-1}$). The complex system of vortices, formed after the contact with the rotating cylinders from the upstream half of the turbine, interacts and influences negatively the cylinders, which are in the downstream half. This is a condition for forming vortex structures, which are then transmitted to the rotating cylinders working on the downstream side of the VAMWT model. Therefore, at the “Challenergy“ company they install rectifying plate after the rotating cylinders.

4 Conclusions

-The present work describes functioning models of HAMWT and VAMWT turbines. Experimental research has been carried out and some measured data of aerodynamic parameters around the operating models have been analyzed;

-HAMWT starts smoothly and works without any problems. The Magnus effect is easily realized. The model is functional if high-quality components are used for its manufacturing. The selection of the number of revolutions and the overall dimensions are problematic, particularly their length. The centrifugal force loads the support frame, which carries the rotating cylinders, however, on the other hand, that force has a stabilizing effect;

- The HAMWT structure has a simpler design and fewer components than the VAMWT structure. That affects the price and the reliability of the unit;

-When air flow across the HAMWT with three cylinders after the rotor there is a turbulent steady flow observed;

-The application of the Magnus effect VAMWT is difficult, yet not impossible. The reason is the complex distribution of the vortices in the area between the rotating cylinders, i.e in the core of the rotating frames. When VAMWT works with two cylinders, a turbulent unsteady flow is observed.

Acknowledgments

The research was done in the Hydro- and Aerodynamics laboratory at TU-Varna. The work described in this paper is the result of a study carried out in project SP16/2023 (HП16/2023) “Aerodynamic analysis of Magnus effect wind turbine” funded by the State Budget.

References

- Al Habib Ullah, Charles Fabijanic, Nick L. Thomas, Bora Suzen, Jordi Estevadeordal. (2022) Experimental investigation of flow past three-cylinder rotating system, *Experimental Thermal and Fluid Science* 142, Elsevier, <https://doi.org/10.1016/j.expthermflusci.2022.110827>
- Anderson, J. (2011) *Fundamentals of Aerodynamics*, 5th ed., McGraw-Hill.
- Shigeru Ogawa, Yusuke Kimura. (2018). Performance Improvement by Control of Wingtip Vortices for Vertical Axis Type Wind Turbine. *Open Journal of Fluid Dynamics*, 8. doi: 10.4236/ojfd.2018.83021
- Prandtl L., O.Titjens. (1934). *Applied hydro-and aeromechanics*. McGraw-Hill
- Willi Bohl, Wolfgang Elmendorf. (2005). *Technische Strömungslehre*, 13. Auflage, Vogel Buchverlag
- Limpot H., Somido A., Yamsuan A., Abuan B., Danao L. (2023). The Performance of a Magnus Vertical Axis Wind Turbine in Typhoon Wind Speeds. *Chemical engineering transactions* Vol.103, <https://doi.org/10.3303/CET23103031>

- Bychkov N., Dovgal A. and Kozlov V. (2007). Magnus wind turbines as an alternative to the blade ones. *Journal of Physics: Conference Series* 75, <https://doi.org/10.1088/1742-6596/75/1/012004>
- Ikezawa Y., Hasegawa H., Ishido T., Haniu T., Murakami N. (2018) Three-dimensional flow field around a rotating cylinder with spiral fin for Magnus wind turbine. *Journal of Flow Visualization and Image Processing*, Volume 25, Issue 1, 2018, pp. 15-24, <https://doi.org/10.1615/JFlowVi-sImageProc.2018026796>
- Borg J. (1986). Magnus effect: An overview of its past and future practical applications. Vol.1 and vol.2.
- Ogawa S., Kimura Y. (2018) Performance Improvement by Control of Wingtip Vortices for Vertical Axis Type Wind Turbine. *Open Journal of Fluid Dynamics*, 8, 331-342. <https://doi.org/10.4236/ojfd.2018.83021>
- Seifert J. (2012). A review of the Magnus effect in aeronautics. *Progress in Aerospace Sciences*. 55, 17-45. <https://doi.org/10.1016/j.paerosci.2012.07.001>
- Tanasheva N.K., Bakhtybekova A.R., Sakipova S.E., Minkov L.L., Shuyushbaeva N.N., Kasimov A.R. (2021) Numerical simulation of the flow around a wind wheel rotating cylindrical blades, <https://doi.org/10.31489/2021No1/51-56>
- Sakipova S.E., Tanasheva N.K. (2019) Modeling aerodynamics of the wind turbine with rotating cylinders. ISSN 1811-1165 (Print) ISSN 2413-2179 (Online) *Eurasian Physical Technical Journal*, Vol.16, No.1(31)
- Tujarov K., Nikolaev I. (2005) [Тужаров К., Николаев И. Измерване на малки въртящи моменти при опитно изпитване на моделни ветроколела, Трудове на юбилейна научна конференция 2005], Vol.44, ser.1, p.238-241, ISSN 1311-3321
- Ahmedov (2013) [Ахмедов А. Методика за изследване на ветроколела с вертикална ос на въртене. Научни трудове на Русенския университет, 2013] vol.52, ser.1.2. <https://conf.uni-ruse.bg/bg/docs/cp13/1.2/1.2-20.pdf>
- Lukin (2022) [Лукин А.Е. Исследование и разработка системы управления ветроэнергетической установкой на эффекте Магнуса, Автореферат] <https://www.dissercat.com/content/issledovanie-i-razrabotka-sistemy-upravleniya-vetroenergeticheskoi-ustanovkoi-na-effekte-mag>
- Testo (2022) Testo 400-Universal IAQ instrument-instruction
- Testo (2023) Kalibrier-Protokoll Hot Wire Probe Head
- DT Digital tachometer DT-2234A Operational manual

Online sources

- Challenergy Inc. (2020) Challenergy's Next-Generation Wind Turbine successfully generated power during Typhoon Hagupit, sets a new record at 30.4 m/s https://challenergy.com/en_b/news/2b0fd3741b9eb2ffb16c98c89b463b676e680a01.pdf
- Challenergy (2024) <https://challenergy.com/en/magnus/#results>